One-Micron-Thick Organic Indoor Light Harvesters with Low Photocurrent Loss and Fill Factors over 67%

Tong Wang[a], Zhen-Chuan Wen[a], Liu-Hong Xu[b], Chao-Chao Qin[b], Hang Yin[*,a], Jian-Qiang Liu[*,a], Xiao-Tao Hao[*,a,c]

[a]School of Physics, State Key Laboratory of Crystal Materials, Shandong University, Jinan, Shandong, 250100, P. R. China.
E-mail: hyin@sdu.edu.cn; jqliu@sdu.edu.cn; haoxt@sdu.edu.cn

[b] Henan Key Laboratory of Infrared Materials and Spectrum Measures and Applications, School of Physics, Henan Normal University, Xinxiang, Henan, 453007, P. R. China.

[c]ARC Centre of Excellence in Exciton Science, School of Chemistry, The University of Melbourne, Parkville, Victoria, 3010, Australia

*Corresponding authors.
E-mail addresses: hyin@sdu.edu.cn (Hang Yin), jqliu@sdu.edu.cn (Jian-Qiang Liu), haoxt@sdu.edu.cn (Xiao-Tao Hao)

Materials and Methods

Materials: The polymer donor PBDB-T, polymer acceptor N2200 and electron transportation layer material PDIN used in this work are purchased from Solarmer Materials, Inc. The insulating polymer polystyrene (PS) was purchased from Sigma-Aldrich Corporation.

The fabrication of OPV devices with different thickness: The device structure of ITO/PEDOT:PSS/active layer/PDIN/Al was used in this work. The ITO substrates with sheet resistance of 15 Ω square^{-1} were cleaned in deionized water, acetone, and isopropanol with ultrasonic treatment for 15 min. And then, the ultraviolet–ozone is used to treat the ITO substrates for 15 min. The PEDOT:PSS solution (PEDOT:PSS : deionized water is 1:1) was spin cast on ITO with 4000 rpm for 50 s to prepare the hole transportation layer. Next, the ITO substrates with PEDOT:PSS were baked in air for 15 min, and then, the samples were moved immediately into the glove box filled with nitrogen. The PBDB-T:N2200 (the concentration ratio was 1:1.2) with 1 vol% 1,8-diodooctane (DIO) chloroform (CF) solution and corresponding diluted blend CF solution with different PS fractions (0-20%), which were stirred for 12h at 60℃, were spin cost on PEDOT:PSS layer with 400-4000 rpm to obtain active layer with different thickness. After the annealing treatment of resulting active layer with 90℃ for 10 min, the PDIN methanol solution (2 mg mL^{-1}) with 0.3 vol% AceticAcid was spin on the active layer with 5000 rpm for 30s. Then, Al cathode (100 nm) was deposited on the PDIN layer via evaporation in vacuum. Finally, OSCs with an effective area of 0.1225

cm^2 were obtained. The current density–voltage (J–V) curve was measured under AM 1.5 illumination of 100 Mw cm^{-2}, LED indoor light (the color temperature is 2700 K) with light power of 1200, 1000 and 500 lux by Keithley 2400 source meter unit. More than 10 devices were fabricated to ensure the reproducibility of the data. Furthermore, the 7-SCSpec system (Sofn Instrument Co. Ltd.) was used to investigate the EQE of OSCs in air.

The calculation of dielectric constant (ε): The geometric capacitance (Cg) is obtained at 1 MHz from frequency-capacitance spectrum, when the capacitance is independent of the frequency. The ε value is calculated by the equation of $\varepsilon = \frac{C_g d}{\varepsilon_0 A}$, where d is the active layer thickness, ε_0 is vacuum dielectric constant and A is the area of device

The calculation of trap density (N_t): The deep trap state can be studied at low-frequency response. Here, the additional capacitance at applied voltage (V) close to build-in voltage (V_{BI}) is assumed to be caused by trapped carriers being releasing to the mobility edge. The trapped charge density of accessible trap state can be calculated according to the correlation as follow,

$$\frac{1}{C^2} \propto -\frac{2}{N_t \varepsilon q A^2}$$

Where C is the capacitance and q is elementary charge.

The calculation of energy disorder (σ): According to Gaussian disorder model (GDM), the low field mobility can be defined as

$$\mu_0 = \mu_\infty \exp[- (\frac{2\sigma}{3KT})^2]$$

where μ_∞ is the high-temperature limit mobility, K is boltzmann constant and T is the temperature.

The measurement of time-resolved photoluminescence (TRPL): For the TRPL, the data were obtained by FLIM (Nanofinder FLEX2. Tokyo Instruments, Inc) with time-correlated single-photo counting (TCSPC) module. The wavelength of 400 nm was selected to excite the sample, and the dynamics of 700 nm was probed in this work.

The measurement of transient absorption (TA) spectrum: The measurement of femtosecond transient absorption spectra was measured with an optical instrument consisted of a Ti:sapphire femtosecond laser (coherent) and an optical parametric amplifier (OPA) system. Seed pulses with 35 fs pulse width and a repetition rate of 1 kHz are generated from the amplified Ti:sapphire femtosecond laser. The seed pulses were split into two parts of laser, one for routing to the OPA to provide a 400 and 750 nm pump pulse that were used in this work and the other for generating a broad band

of 520–800 nm (visible) and 850–1300 nm (NIR) probe light. The energy of the excitation beam was 18 nJ pulse^{-1}, which is too low to generate the annihilation effects of exciton–exciton and exciton–charge.

Exciton dissociation probability (P(E,T)): P(E,T) was obtained from the correlation of photocurrent (J_{ph}) and effective voltage (V_{eff}) of the OSCs. The value of J_{ph} is determined by the equation of $J_{ph}=J_L-J_D$ (J_L and J_D represent the current densities under light and in the dark, respectively). V_{eff} is determined by the equation of $V_{eff}=V_0-V_a$ (V_0 is the voltage at which J_{ph} is equal to zero, V_a is the applied bias voltage). The J_{ph} will saturates at a high V_{eff} (i.e., V_{eff}=2 V), and the corresponding current density is defined as J_{sat}. Through the equation of $J_{sat}=qG_{max}L$ (q is the electronic charge, L is the active layer thickness), G_{max} values can be calculated. Additionally, the value of P(E,T) is obtained from the ratio of J_{ph}/J_{sat} under short-circuit condition.

The measurement of grazing incidence X-ray diffraction (GXRD): GIXD characterizations were performed at the BL14B1 beamline of the Shanghai Synchrotron Radiation Facility (SSRF) in China. The distances of sample-to-detector, incidence light angle and wavelength are 352 mm, 0.16° and 0.124 nm, respectively.

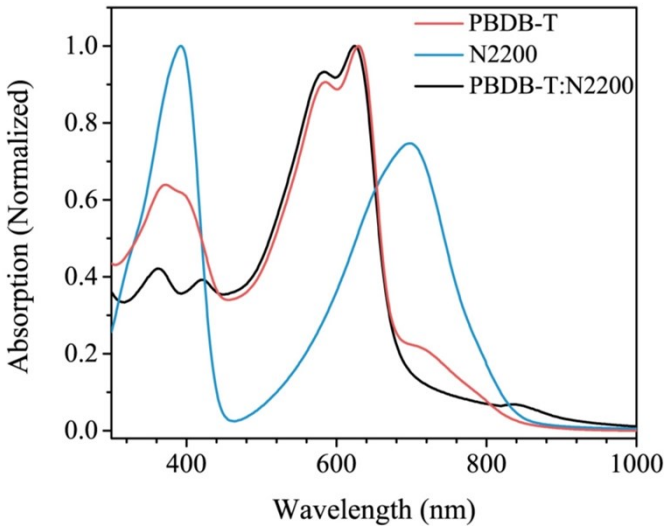

Figure S1. The absorption spectra for PBDB-T, N2200 and PBDB-T:N2200 blend.

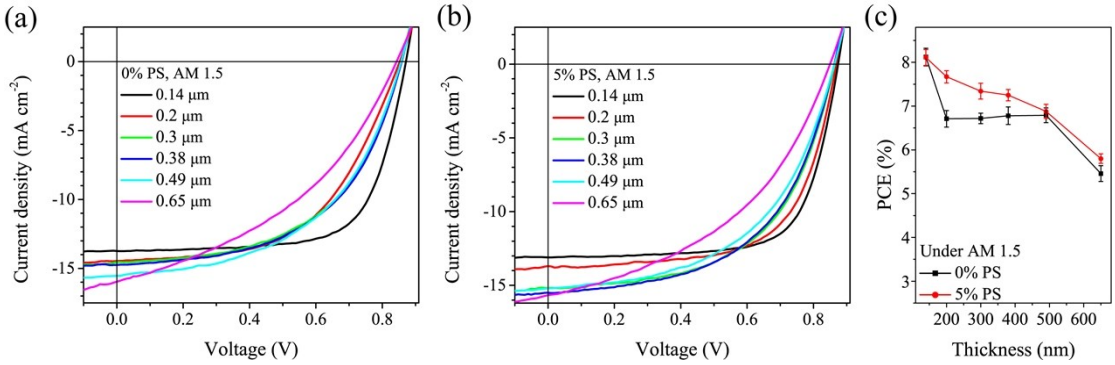

Figure S2. The current density (J)-voltage (V) curves for (a) no-diluted and (b) 5% PS-diluted devices with different active layer thickness under AM 1.5. (c) The PCE versus active layer thickness under AM 1.5.

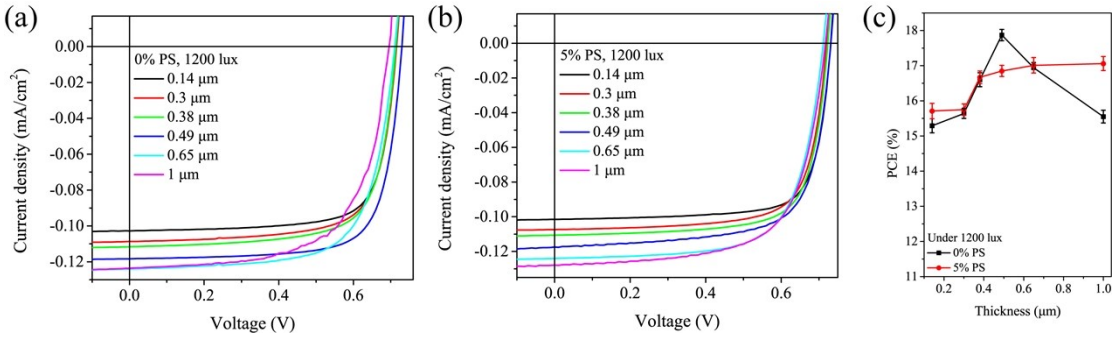

Figure S3. The current density (J)-voltage (V) curves for (a) no-diluted and (b) 5% PS-diluted devices with different active layer thickness under LED light with 1200 lux and 2700 K. (c) The PCE versus active layer thickness under LED light with 1200 lux and 2700 K.

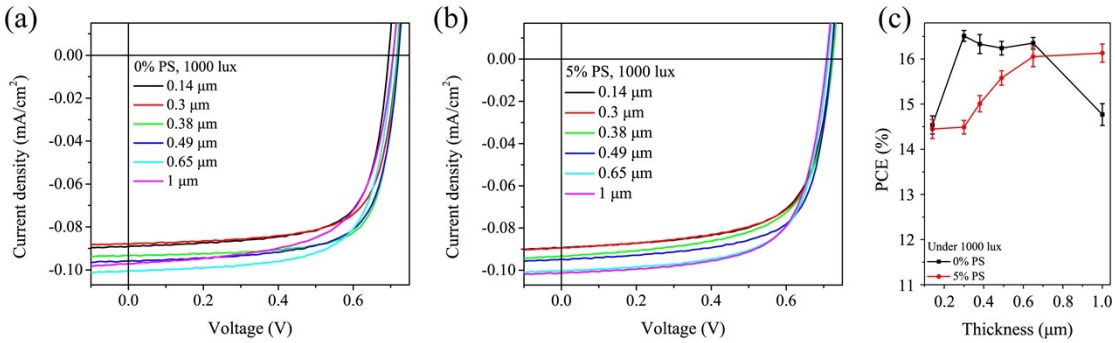

Figure S4. The current density (J)-voltage (V) curves for (a) no-diluted and (b) 5% PS-diluted devices with different active layer thickness under LED light with 1000 lux and 2700 K. (c) The PCE versus active layer thickness under LED light with 1000 lux and 2700 K.

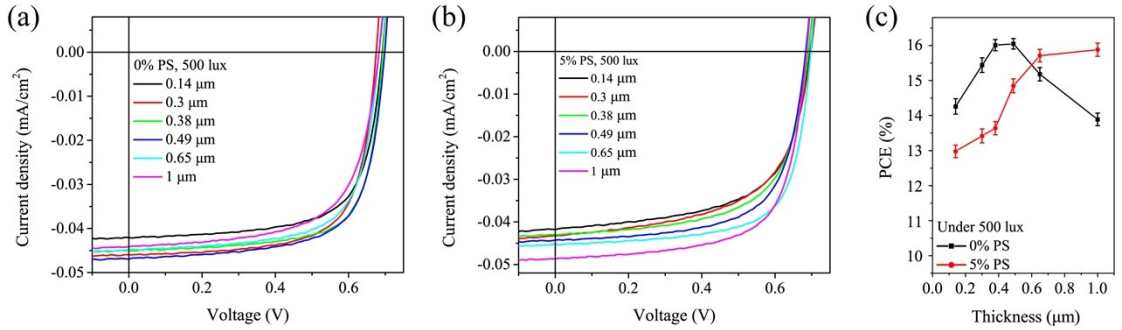

Figure S5. The current density (J)-voltage (V) curves for (a) no-diluted and (b) 5% PS-diluted devices with different active layer thickness under LED light with 500 lux and 2700 K. (c) The PCE versus active layer thickness under LED light with 500 lux and 2700 K.

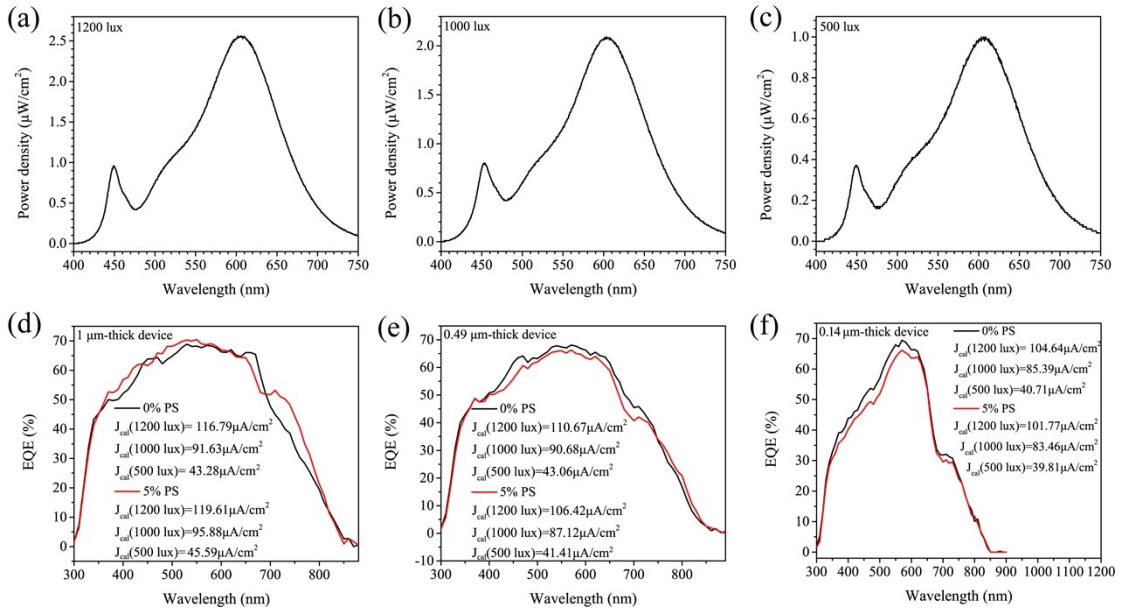

Figure S6. Light power density under different wavelength for LED light with (a) 1200 lux, (b) 1000 lux and (c) 500 lux. EQE spectra for (d) 1 μm-thick , (e) 0.49 μm-thick and (f) 0.14 μm-thick devices, and the calculated short-circuit current density (J_{cal}) under 1200, 1000 and 500 lux LED light are listed in the corresponding figures.

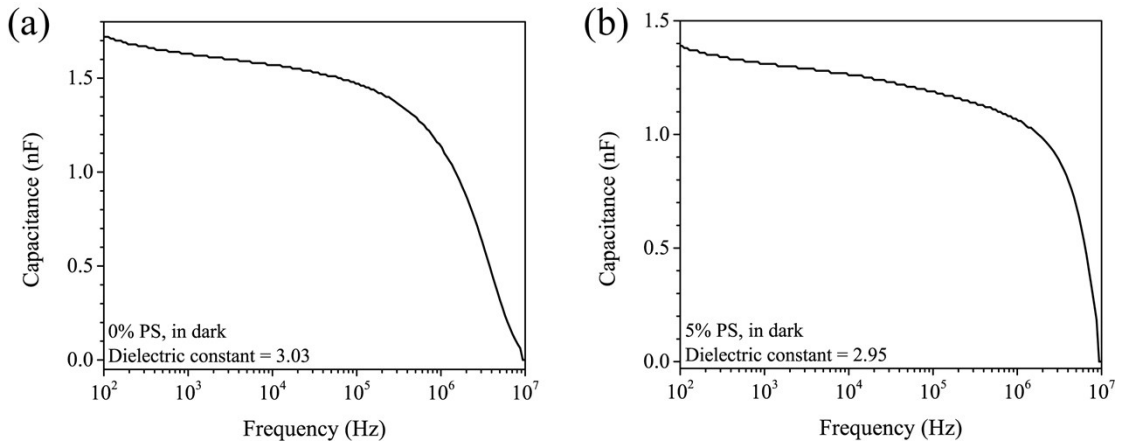

Figure S7. The frequency-dependent capacitance for (a) PBDB-T:N2200 and (b) diluted PBDB-T:N2200 with 5% PS in dark.

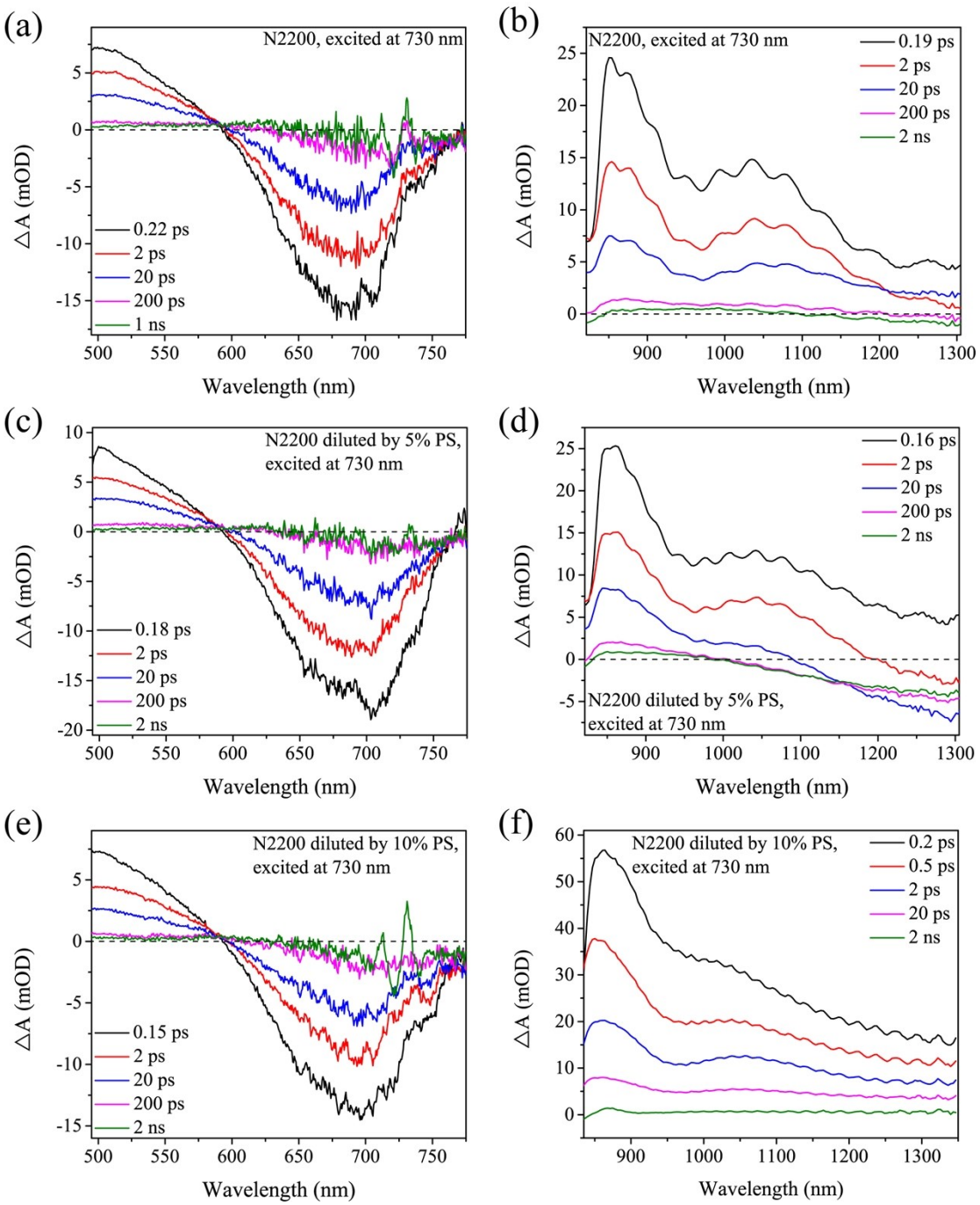

Figure S8. The TA spectra probed at (a) visible (Vis) and (b) near infrared (NIR) region for neat N2200. The TA spectra probed at (c) visible (Vis) and (d) near infrared (NIR) region for N2200:PS (5%). The TA spectra probed at (e) visible (Vis) and (f) near infrared (NIR) region for N2200:PS (10%).

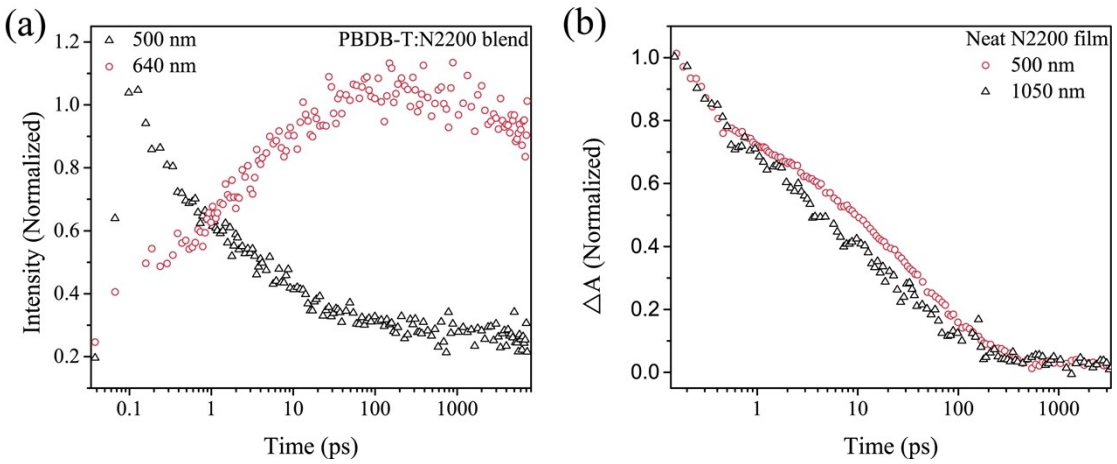

Figure S9. (a) The dynamics of ESA signal at 500 nm and GSB signal at 640 nm for PBDB-T:N2200 blend. (b) The dynamics of ESA signal at 500 and 1050 nm for N2200 film.

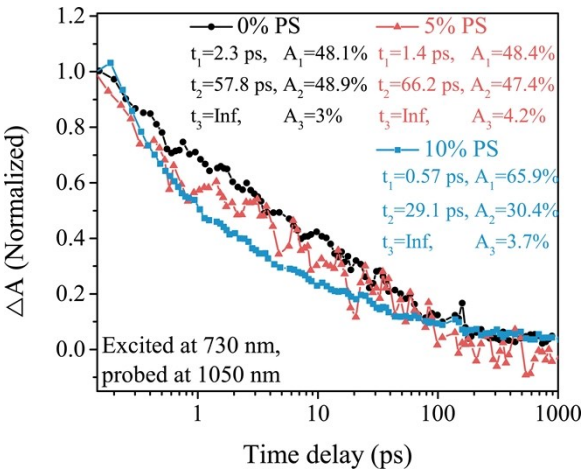

Figure S10. The TA dynamics of the N2200 films with 0%, 5% and 10% PS probed at 1050 nm.

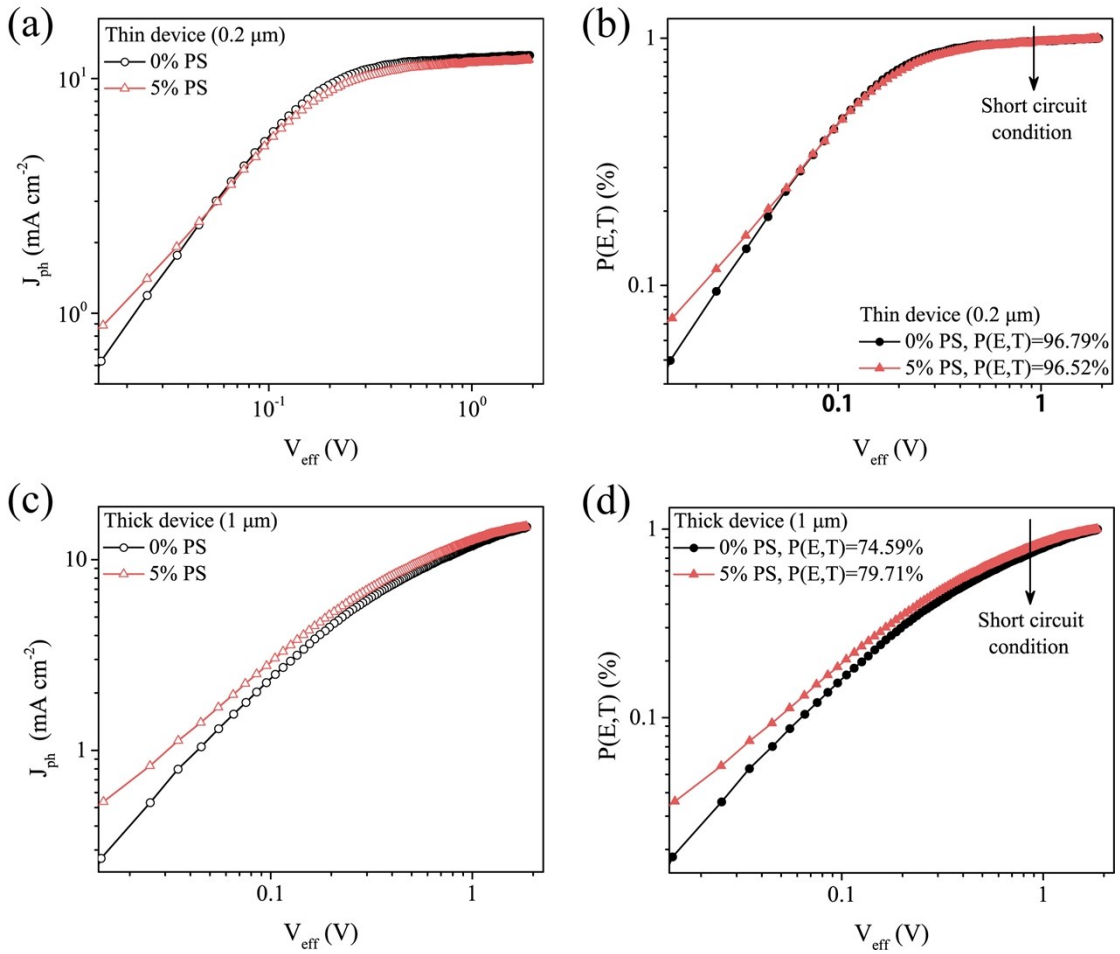

Figure S11. The effective voltage dependent (a) J_{ph} and (b) P(E,T) for 0.2 μm devices. The effective voltage dependent (c) J_{ph} and (d) P(E,T) for 1 μm devices.

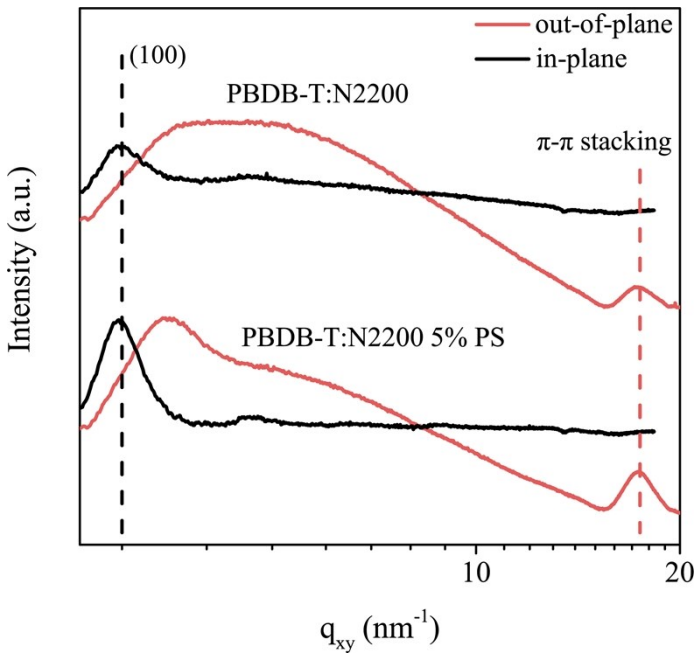

Figure S12. The line-cut profiles from GIXRD patterns along out-of-plane and in-plane for PBDB-T:N2200, PBDB-T:N2200:PS (5%).

Table S1. The detailed device parameters for PBDB-T:N2200 and PBDB-T:N2200:PS (5%) devices with different active layer thickness under AM 1.5.

	Thickness (nm)	J_{SC} (mA/cm^2)	V_{OC} (V)	FF (%)	PCE (%)
0%	140	13.74 (±0.24)	0.86 (±0.001)	68.78 (±0.50)	8.12 (±0.20)
	200	14.47 (±0.13)	0.85 (±0.001)	54.35 (±0.64)	6.71 (±0.19)
	300	14.53 (±0.15)	0.86 (±0.002)	53.99 (±0.6)	6.72 (±0.12)
	380	14.75 (±0.16)	0.86 (±0.001)	53.55 (±0.56)	6.78 (±0.20)
	490	15.53 (±0.11)	0.86 (±0.001)	51.04 (±0.45)	6.79 (±0.17)
	650	15.97 (±0.12)	0.84 (±0.001)	40.56 (±0.42)	5.46 (±0.15)
5%	140	13.11 (±0.13)	0.88 (±0.002)	70.31 (±0.40)	8.11 (±0.18)
	200	13.70 (±0.10)	0.87 (±0.001)	64.50 (±0.81)	7.64 (±0.14)
	300	15.19 (±0.13)	0.86 (±0.001)	55.91 (±0.53)	7.34 (±0.18)
	380	15.50 (±0.12)	0.86 (±0.001)	54.19 (±0.70)	7.25 (±0.13)
	490	15.20 (±0.17)	0.86 (±0.001)	52.45 (±0.66)	6.88 (±0.16)
	650	15.67 (±0.14)	0.85 (±0.20)	43.50 (±0.45)	5.80 (±0.16)

Table S2. The detailed device parameters for PBDB-T:N2200 and PBDB-T:N2200:PS (5%) devices with different active layer thickness under LED light with 1200 lux and 2700 K.

	Thickness (nm)	J_{SC} (μA/cm^2)	V_{OC} (V)	FF (%)	PCE (%)
0%	140	102.75 (±1.38)	0.71 (±0.001)	75.02 (±0.50)	15.29 (±0.20)
	300	108.69 (±1.06)	0.72 (±0.002)	72.43 (±0.71)	15.64 (±0.14)
	380	116.39 (±1.20)	0.71 (±0.002)	71.95 (±0.51)	16.60 (±0.20)
	490	118.34 (±0.85)	0.73 (±0.003)	74.47 (±0.52)	17.87 (±0.16)
	650	124.03 (±1.03)	0.71 (±0.001)	69.17 (±0.80)	16.94 (±0.15)
	1000	123.60	0.70	65.09	15.55

		(±0.95)	(±0.001)	(±0.65)	(±0.18)
5%	140	101.49	0.73	76.16	15.71
		(±1.14)	(±0.002)	(±0.42)	(±0.22)
	300	107.43	0.72	73.25	15.75
		(±1.06)	(±0.002)	(±0.42)	(±0.16)
	380	110.68	0.72	73.60	16.67
		(±0.91)	(±0.001)	(±0.60)	(±0.18)
	490	117.34	0.73	70.65	16.85
		(±1.02)	(±0.002)	(±0.72)	(±0.16)
	650	124.09	0.71	69.33	17.01
		(±0.75)	(±0.002)	(±0.64)	(±0.22)
	1000	127.80	0.72	67.01	17.06
		(±1.17)	(±0.001)	(±0.68)	(±0.20)

Table S3. The detailed device parameters for PBDB-T:N2200 and PBDB-T:N2200:PS (5%) devices with different active layer thickness under LED light with 1000 lux and 2700 K.

	Thickness (nm)	J_{SC} (μA/cm^2)	V_{OC} (V)	FF (%)	PCE (%)
0%	140	89.08	0.70	70.46	14.54
		(±0.82)	(±0.001)	(±0.60)	(±0.20)
	300	93.24	0.72	74.12	16.51
		(±0.70)	(±0.002)	(±0.71)	(±0.12)
	380	93.23	0.72	73.50	16.33
		(±0.60)	(±0.001)	(±0.62)	(±0.21)
	490	95.87	0.72	70.49	16.24
		(±0.91)	(±0.001)	(±0.66)	(±0.15)
	650	100.65	0.71	68.91	16.35
		(±0.54)	(±0.001)	(±0.85)	(±0.13)
	1000	97.04	0.71	64.64	14.77
		(±0.74)	(±0.002)	(±0.80)	(±0.24)
5%	140	89.36	0.72	67.30	14.45
		(±0.62)	(±0.001)	(±0.78)	(±0.21)
	300	89.34	0.72	67.41	14.49
		(±0.61)	(±0.001)	(±0.60)	(±0.15)
	380	93.15	0.72	66.73	15.01
		(±0.66)	(±0.002)	(±0.72)	(±0.18)
	490	94.41	0.72	68.71	15.58
		(±0.98)	(±0.002)	(±0.72)	(±0.16)
	650	100.29	0.71	67.45	16.05
		(±0.72)	(±0.001)	(±0.64)	(±0.22)
	1000	101.24	0.71	67.31	16.13
		(±0.86)	(±0.001)	(±0.68)	(±0.20)

Table S4. The detailed device parameters for PBDB-T:N2200 and PBDB-T:N2200:PS

(5%) devices with different active layer thickness under LED light with 500 lux and 2700 K.

	Thickness (nm)	J_{SC} (μA/cm^2)	V_{OC} (V)	FF (%)	PCE (%)
0%	140	42.04 (±0.76)	0.69 (±0.001)	68.60 (±0.62)	14.26 (±0.22)
	300	45.94 (±0.89)	0.68 (±0.001)	69.65 (±0.52)	15.44 (±0.21)
	380	44.97 (±0.78)	0.69 (±0.001)	71.89 (±0.81)	16.01 (±0.16)
	490	46.91 (±0.85)	0.70 (±0.002)	68.56 (±0.54)	16.05 (±0.15)
	650	45.10 (±0.71)	0.68 (±0.002)	69.01 (±0.46)	15.18 (±0.19)
	1000	44.13 (±0.76)	0.68 (±0.001)	64.52 (±0.68)	13.89 (±0.18)
5%	140	41.90 (±0.89)	0.70 (±0.002)	62.30 (±0.60)	12.98 (±0.18)
	300	44.10 (±0.72)	0.70 (±0.002)	61.00 (±0.72)	13.42 (±0.20)
	380	43.01 (±0.62)	0.69 (±0.001)	64.21 (±0.64)	13.64 (±0.19)
	490	44.96 (±0.74)	0.69 (±0.001)	67.01 (±0.89)	14.85 (±0.20)
	650	45.22 (±0.88)	0.70 (±0.002)	69.64 (±0.82)	15.71 (±0.18)
	1000	48.68 (±0.82)	0.69 (±0.001)	66.50 (±0.78)	15.88 (±0.19)

Table S5. The detailed fitted data for TA dynamics of PBDB-T:N2200 and PBDB-T:N2200:PS (5%) probed at 500 nm.

	t1 (s)	A1 (%)	t2 (s)	A2 (%)	t3 (s)	A3 (%)	t4 (s)	A4 (%)
0% PS	0.19	44.9	5.5	25.5	137.0	8.4	Inf	21.2
5% PS	0.16	46.4	4.2	23.1	199.0	10.8	Inf	19.7